Curious cross-field transport effects in multi-ion, magnetized plasma

Cite as: Phys. Plasmas **31**, 112303 (2024); doi: 10.1063/5.0227736
Submitted: 10 July 2024 · Accepted: 25 October 2024 ·
Published Online: 21 November 2024

M. E. Mlodik[a] and N. J. Fisch

AFFILIATIONS

Department of Astrophysical Sciences, Princeton University, Princeton, New Jersey 08543, USA

Note: This paper is part of the Special Collection: Papers from the 65th Annual Meeting of the APS Division of Plasma Physics.
Note: Paper UI4 1, Bull. Am. Phys. Soc. **68** (2023).
[a]Invited speaker. **Author to whom correspondence should be addressed:** mmlodik@princeton.edu

ABSTRACT

In contrast to single-ion plasma, multiple-ion-species plasma exhibits new, curious, and large transport effects. On short timescales, where ions exchange momentum, magnetized multi-ion plasma behaves as a most unusual substance, compressible across field lines in number density but incompressible in charge density. It takes 40 times longer for electrons to participate. In this ion–ion cross-field transport regime, we identified the charge-incompressibility heat pump effect, transferring heat both spatially and between species. Curiously, the direction of impurity transport strongly depends on plasma magnetization, characterized by the ratio of light ion gyrofrequency to the collision frequency between light and heavy ion species. The expulsion of heavy ion impurities from a hotspot occurs sufficiently quickly to be observable on MagLIF, so long as plasma becomes sufficiently collisionally magnetized under implosion. Even more curious, multi-ion transport changes its nature in partially ionized plasma, where ions occupy different charge states. In this regime, we identify a partial-ionization deconfinement effect. The combination of cross-field transport, ionization, and recombination leads to a net ion charge moving across magnetic field lines on the ion–ion transport timescale as opposed to the electron–ion transport timescale. Cross-field transport effects in multi-ion plasma are important in a number of applications, including nuclear fusion and plasma mass filters.

I. INTRODUCTION

Plasma is a rich medium that allows many degrees of freedom and types of interactions, stemming, in part, from the fact that plasma is generally comprised of both positively and negatively charged species. However, for plasma consisting of multiple ion species, even more degrees of freedom and, with that, even more possibilities for new phenomena are opened up. In particular, this richness of physics shows up in cross-field transport in magnetized plasma.

Here, we analyze and present several new and curious transport effects in multi-ion, magnetized plasma, focusing on several effects recently uncovered by us.[1–3] These fundamental effects can be manifested within a wide range of laboratory plasmas, from tokamaks and mirror machines to Z-pinches. Here, we explore the commonalities of these curious, multi-ion transport effects, providing an overarching and didactic perspective. Additionally, we propose how these effects might be observed in laboratory settings.

There are three key observations to be made that can help us to understand cross-field transport in multi-ion magnetized plasmas:

First, observe that it is hard to push charge across magnetic field lines. Canonical momentum $m\mathbf{v} + q\mathbf{A}$ conservation implies that in order to push charge across field lines, an input of momentum is required (here, m is the particle mass, q is the charge, $\mathbf{v}$ is the velocity, and $\mathbf{A}$ is the magnetic vector potential). If there is no input of momentum in a given process (for example, in a collision), then net charge is not pushed across the magnetic field.

Second, observe the following: if plasma is comprised of different species, then different species may react differently to an external stimulus, be it an imposed potential, a temperature gradient, or a density gradient, at different timescales. Therefore, plasma allows timescale separation, in which some species react to that external stimulus while other species do not react. In particular, in the case of cross-field transport, the friction force between different species is crucial. For plasma far out of thermodynamic equilibrium, the ion–ion friction force tends to be much larger than the electron–ion friction force, so multi-ion transport processes tend to dominate.

Third, observe that plasma has a peculiar response to temperature gradients, owing to the scaling of collision frequency with velocity in plasma.[4–8] This response can be understood by looking at a heavy test particle in the following way. In unmagnetized plasma, particles coming from a hotter region collide less with the test particle than particles coming from a colder region, resulting in a thermal force which pushes the test particle toward the hotter region. In other areas of physics, this is known as the *Nernst effect*. In magnetized plasma, the thermal force is perpendicular to both the temperature gradient and the direction of the magnetic field. In turn, this thermal force in magnetized plasma leads to $\mathbf{F}\times\mathbf{B}$ drift, which pushes a test particle toward the colder region. There is also an Onsager-symmetric counterpart to the thermal force, which is called the *Ettingshausen effect*. Colder particles collide more frequently than do hotter particles. Therefore, for plasma nearly in local temperature equilibration, if there is a particle flux driven by collisions, then it would be disproportionately a flux of cold particles, which appears as a heat flux in the opposite direction.

Taken together, these observations will be instrumental in categorizing and understanding multi-ion transport in magnetized plasma in a variety of plasma regimes and in a variety of applications. It is the objective here to explore how these observations play a role in uncovering a number of very curious and new effects.

The paper is organized as follows. In Sec. II, equilibrium in fully ionized, fully magnetized plasma is considered and heat pump effect is shown. In Sec. III, partially magnetized plasma is considered and pinch reversal effect is shown. In Sec. IV, possible experiments to validate the pinch effect are discussed. In Sec. V, plasma with ions in multiple charge states is considered and a partial-ionization deconfinement effect is shown. Section VI provides a summary and discussion of various approaches to the study of multi-ion transport effects, as well as future directions which may help to uncover even more multi-ion transport effects.

II. GENERALIZED PINCH EQUILIBRIUM. HEAT PUMP EFFECT

Cross-field transport has different properties depending on what kind of plasma is considered. In this section, we look at the basic scenario of fully ionized and magnetized plasma. In subsequent sections, we relax these assumptions and identify how the transport behavior changes.

Suppose that there is a magnetized plasma slab, with uniform magnetic field in the z-direction, and all the gradients in the x-direction, as depicted in Fig. 1. Then, cross-field transport in the x-direction is equivalent to an $\mathbf{F}\times\mathbf{B}$ drift generated by the forces acting in the y-direction. Note that the larger the force is, the larger the particle flux corresponding to the force is too. There are only a few forces acting in the y-direction if all the gradients are in the x-direction. Both ion–ion and electron–ion friction forces are examples of those forces. Note that, if the plasma is far from thermodynamic equilibrium, then in general, the ion–ion friction force is much larger than electron–ion friction force. Therefore, the ion–ion cross-field transport timescale is much faster than the electron–ion cross-field transport timescale, $\tau_{ii,eq}/\tau_{ei,eq}=\mathcal{O}((1/Z_i)\sqrt{m_e/m_i},\beta)\ll 1$, electrons move across magnetic field lines much less than ions on the ion–ion transport timescale, and net ion charge density is approximately conserved, if plasma $\beta=nT/(B^2/(2\mu_0))\ll 1$. Here, m_s is the mass of species s, Z_i is the charge state of ion species i, n is the plasma number density, T is the plasma temperature, B is the magnetic field strength, and μ_0 is the vacuum permeability.

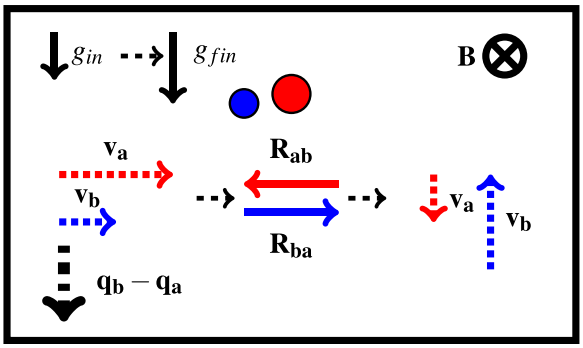

FIG. 1. The cause of ion cross-field transport. Change in g leads to the difference in ion drift velocities, which produces frictional drift in vertical direction. Ions with higher m/Z (red) move toward the bottom, while ions with lower m/Z (blue) move to the top. Note that there is no net ion charge motion across field lines. Difference in ion drift velocities also makes heat flux to appear (Ettingshausen effect).

This timescale separation means that the ion density profiles equilibrate between themselves faster than with electrons. In the absence of any temperature gradient, equilibrium between ion species requires[9–12]

$$(n_a e^{\Phi_a/T})^{1/Z_a}\propto(n_b e^{\Phi_b/T})^{1/Z_b}, \tag{1}$$

where Φ_s is the potential energy of an ion of species s, n_s is the density of species s, and Z_s is the charge of species s. Φ_s can include any potentials present in the system, including electrostatic, gravitational, and centrifugal potentials. Behavior of this kind has been predicted and observed in a variety of contexts.[13–27] These density relations are called *generalized pinch relations*. They have the following properties. First, if $\Phi_a=\Phi_b=0$, then higher-Z species are concentrated ("pinched") very strongly in the highest-density region of the plasma, satisfying $n_b\propto n_a^{Z_b/Z_a}$. Second, relations in Eq. (1) are satisfied for pair of species $b-c$ if they are satisfied for pairs $a-b$ and $a-c$, so the generalized pinch relations possess transitivity. Interestingly, the generalized pinch relations are the maximum-entropy state of the plasma subject to the constraints that only species that obey the relations can move across magnetic field lines on a given timescale and that cross-field transport does not move net charge across field lines.[28,29] And, last but not least, if there are k ion species in the plasma, Eq. (1) provides $k-1$ constraints. In order to determine actual densities of plasma constituents, another constraint is needed. Therefore, density profiles that satisfy generalized pinch relations can look quite different. One solution to Eq. (1) is Gibbs equilibrium, $n_s\propto\exp(-\Phi_s/T)$ for all species s.

Another solution that satisfies generalized pinch relations is the following. Suppose that the potential Φ_s in Eq. (1), such as a centrifugal potential, changes. Then, on the ion–ion transport timescale, electron density does not change, while ion densities change until they equilibrate with each other and can be described by generalized pinch relations. In this case, electron density is approximately conserved on the ion–ion transport timescale. Net ion charge density is approximately conserved too because of plasma quasineutrality. Combined together, this results in ion separation on the ion–ion transport timescale. This ion separation is not the only thing that happens to plasma if the

potential Φ is changed. Net ion density can change even though net ion *charge* density is conserved, so the plasma is heated in some places and cooled in the other places. Note, however, that cross-field particle flux is accompanied by heat flux (Ettingshausen effect), because cold ions move across magnetic field lines more easily than hot ions. These two processes have the same scaling, and the net result usually is that the region of plasma where high-Z ions move to gets heated and the right where low-Z ions move to gets cooled. The amount of heating is proportional to the change in potential energy and is a fraction of it (see Ref. 1 for details). This effect of redistribution of heat within plasma due to multi-ion cross-field transport is called *heat pump effect in magnetized plasma*.

One potential area of application of this effect is plasma mass filters, devices designed to separate ion species based on their mass.[19,20,25,26,30–41] However, other multi-ion cross-field transport effects are applicable to even more kinds of plasma. We will explore them in the subsequent sections.

III. PARTIAL MAGNETIZATION. PINCH REVERSAL EFFECT

The plasma response to a species-dependent external force $\mathbf{F}_s$ in the direction perpendicular to magnetic field $\mathbf{B}$ depends on the strength of the magnetic field. There are two dimensionless parameters that govern the type of the response of species s to that force, namely, Larmor magnetization ρ_s/L and collisional magnetization Ω_s/ν_s. Here, ρ_s is the Larmor radius of species s, L is the characteristic length scale in the direction perpendicular to the magnetic field, Ω_s is the gyrofrequency of species s, and ν_s is the collision frequency of species s. In the case when plasma is unmagnetized ($\rho_s/L \gg 1$, $\Omega_s/\nu_s \ll 1$), the response to an external force is acceleration, i.e., $d_s\mathbf{u}_s/dt \propto \mathbf{F}_s$, where $\mathbf{u}_s$ is the flow velocity of species s, $d_s/dt = \partial/\partial t + \mathbf{u}_s \cdot \nabla$. In the case when plasma is magnetized ($\rho_s/L \ll 1$, $\Omega_s/\nu_s \gg 1$), the response of species s to an external force is drift velocity, i.e., $\mathbf{u}_s = \mathbf{F} \times \mathbf{B}/(q_s B^2)$.

There is a subtlety with what collision frequency to choose. If there is a large mass disparity between two species a and b such that $m_a \ll m_b$, then the correct Hall parameter for the purpose of multi-ion transport is Ω_a/ν_{ab}. More generally, in the case of large mass disparity between ions, the ion–ion transport coefficients can be inferred from the electron–ion transport coefficients with the substitutions $\overline{Z} \to (n_b Z_b^2)/(n_a Z_a^2)$ and $\omega\tau \to \Omega_a/\nu_{ab}$, where $\omega\tau$ is the electron Hall parameter and $\overline{Z}$ is the effective ion charge for the purpose of electron–ion transport. Note that recently there have been developments in accurate determination of electron–ion transport coefficients.[42–45]

Timescale separation works slightly differently in partially magnetized plasma as opposed to magnetized plasma. If plasma is collisionally unmagnetized but $\Omega_e \gg \nu_{ei}$, then the multi-ion transport timescale scales like $\tau_{ab,eq} \propto \nu_{ab} L^2/v_{th,i}^2$, while the electron–ion transport timescale scales like $\tau_{ei,eq} \propto (\Omega_i^2/\nu_{ie})(L^2/v_{th,i}^2)$, where $v_{th,i}$ is the ion thermal velocity, $\nu_{ei} = \nu_{ea} + \nu_{eb}$ is the collision frequency of electrons with all kinds of ions, and L is the characteristic length scale perpendicular to the magnetic field. Therefore, the timescale separation described in Sec. II occurs in partially magnetized plasma if $(\Omega_a/\nu_{ab})(\Omega_e/\nu_{ei}) \gg 1$.

In partially magnetized plasma, the relationship between ion densities in equilibrium (in the absence of additional external potentials Φ_s) is

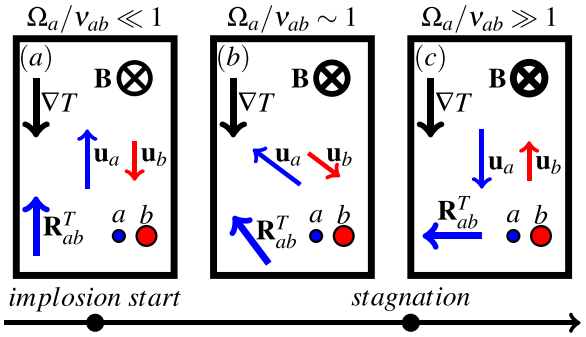

FIG. 2. Time history of MagLIF implosion from plasma magnetization standpoint. In the beginning, plasma is collisionally unmagnetized. As implosion progresses, plasma gets more magnetized, becoming collisionally magnetized around stagnation. The reaction of heavy impurity ions to radial temperature gradient switches, resulting in expulsion from the hotspot around stagnation.

$$\frac{1}{Z_b}\left(\frac{n_b'}{n_b}+\frac{T_b'}{T_b}\right)=\frac{1}{Z_a}\left(\frac{n_a'}{n_a}+\frac{T_a'}{T_a}+\lambda\frac{T_a'}{T_a}\right). \tag{2}$$

Here, λ is the temperature screening coefficient and is a function of Ω_a/ν_{ab}. This equation is accurate up to first order in $\mathcal{O}(m_a/m_b)$ and $\mathcal{O}((Z_a m_a)/(Z_b m_b))$. Note that λ is positive if $\Omega_a/\nu_{ab} \ll 1$ and approaches $-3/2$ as Ω_a/ν_{ab} becomes large.

Figure 2 shows the transition between different magnetization regimes which happens during a MagLIF implosion. Note that during a Z-pinch implosion ion Hall parameter increases, and plasma becomes more magnetized. Depending on implosion parameters, it is possible for λ to change sign and for the tendency of high-mass impurities to concentrate to reverse. In particular, a MagLIF implosion is an example of a plasma where this effect can take place. Following Ref. 2, if plasma parameters at stagnation BR $= 0.2\,\mathrm{MG}\cdot\mathrm{cm}$, r $= 60\,\mu\mathrm{m}$ (which corresponds to B $= 3.3\,\mathrm{kT}$), fuel density is $\rho\mathrm{R} = 0.4\,\mathrm{g/cm^2}$, $T_i = 2.6\,keV$ are considered, then the ion Hall parameter is such that plasma is close to being collisionally magnetized, and collisional transport timescale is comparable to the burn time. In particular, if $n_{Be} = 0.01 n_D$, then $\Omega_D/\nu_{D,Be} = 3.75$ and $\tau_{BeD,eq} = 3.7\,ns$. The multi-ion radial transport timescale is comparable to the burn time ($\sim 2\,ns$) and is much smaller than the implosion timescale ($\sim 100\,ns$), so significant impurity transport can be expected to occur. The following section describes how to construct a plasma to be able to observe this pinch reversal effect experimentally.

IV. POSSIBLE EXPERIMENTS

In this section, we show a potential avenue for experimental testing of the pinch reversal effect. In fusion devices, it is typically advantageous to concentrate fuel ions in the hot core of the plasma and to flush out impurities and fusion products.[18,46–52] For example, impurity transport is of interest in MagLIF.[53,54] MagLIF, a large magnetized Z-pinch, features an axial B field, with deuterium plasma heated in the center by a laser and compressed by applying a large current to the beryllium liner. In Sec. III, it was identified that ion density profiles evolve sufficiently fast for radial impurity transport to be significant around stagnation on MagLIF, leading to expulsion of heavy ion impurities from the hotspot as long as plasma becomes sufficiently collisionally magnetized during the implosion, although, in insufficiently

magnetized plasma, the transport effect is reversed. Thus, trace H ions were used on Omega laser facility (unmagnetized) to increase the concentration of DT fuel in the hotspot and reduce demixing of fuel, as heavier ions tend to concentrate in the high-T region of plasma.[55] However, the effect would be opposite in partially magnetized or collisionally magnetized plasma. In that case, the use of H ions would unfortunately lead to increasing fuel concentration in the low-T region of plasma, and heavy ions should be used instead. For similar reasons, using trace high-Z ions to track impurity transport in MagLIF[56] can make qualitatively incorrect predictions if impurities are present in sufficiently large concentrations.

Thus, the reversal of the radial impurity transport effect is a fundamental problem of high practical impact, with subtle features. The direction of radial transport depends on the degree of collisionality of multiple ion species (not all of which are collisional to the same degree), the degree of ionization, and the degree of magnetization. It can reverse direction just on the basis of impurity concentration. However, this multi-ion transport theory has not yet been tested. It is thus an interesting research direction to demonstrate and identify the thresholds for this sign reversal.

A. Suggested experimental strategy

Impurities tend to concentrate in regions of plasma according to change of sign of impurity transport with ion Hall parameter Ω_a/ν_{ab}. When plasma is collisionally magnetized (i.e., $\Omega_a/\nu_{ab} \gg 1$, where a is a bulk ion species and b is a heavy impurity ion species), impurity ions tend to concentrate in colder, denser regions of plasma. When plasma is collisionally unmagnetized (i.e., $\Omega_a/\nu_{ab} \ll 1$, where a is a bulk ion species and b are heavy impurity ions), impurity ions tend to concentrate in hotter, denser regions. Quantitative predictions of the impurity transport reversal effect require ion mass disparity, i.e., $m_a \ll m_b$. The multi-ion transport timescale $\tau_{ab,eq}$ should be sufficiently fast compared to implosion time τ_{imp} at least at some point during the implosion. Aside from that, a strategy to have ions sample variety of ion Hall parameter Ω_a/ν_{ab} values is required, which is possible by using one of the following strategies.

One way to observe the effect would be to use two different impurities. If impurity species b is collisionally unmagnetized $\Omega_a/\nu_{ab} \ll 1$, impurity species c is in trace quantity such that $\Omega_a/\nu_{ab} \gg 1$, and transport timescales are sufficiently fast, i.e., $\tau_{ab,eq} < \tau_{imp}$ and $\min(\tau_{ac,eq}, \tau_{bc,eq}) < \tau_{imp}$, impurity b will concentrate in the hotter region of plasma while impurity c will concentrate in the colder regions. Another way to observe the effect would be to vary impurity density. If the impurity is in trace concentration, the relevant ion Hall parameter is guaranteed to be $\Omega_a/\nu_{ab} \gg 1$, i.e., impurity ions are collisionally magnetized and concentrated in colder regions of plasma. If the impurity is in large concentration, the effect is reversed, even if all the other parameters (such as the current going through the system and the ion temperature) are the same. Yet another way to observe the effect is to have such experimental parameters that the ion Hall parameter increases from $\Omega_a/\nu_{ab} < 1$ to $\Omega_a/\nu_{ab} > 1$ during the compression, as in MagLIF.[2] Impurity ions would initially concentrate in hotter parts of plasma and then move to colder parts of plasma during compression.

In order to see the impurity transport reversal effect, plasma parameters should satisfy the following conditions: one, small ion Larmor orbits, i.e., $\rho_i/r \ll 1$; two, collisionally magnetized electrons, i.e., $\Omega_e/\nu_{ei} \gg 1$; and, three, ion Hall parameter $\Omega_a/\nu_{ab} \lesssim 1$ at some points and $\Omega_a/\nu_{ab} \gtrsim 1$ at other points. The difference can be either for different impurities or for different densities of the same impurity or at different times in the same implosion.

TABLE I. Expressions are normalized by the values similar to initial compression at a Weizmann Institute Z-pinch experiment (oxygen, species a), assuming the presence of trace heavy impurity species b. That is, the temperatures T_a, T_e are normalized to 10 eV, densities n_b to 10^{16} cm^{-3}, n_e to 10^{18} cm^{-3}, mass numbers A_a and A_b to 16, charge states Z_a and Z_b to 4, r to 1 mm, B to 1 T, and the Coulomb logarithms to 5. Multi-ion transport timescale, electron and ion Hall parameters are presented in the case of trace heavy impurity.

Quantity	Normalized expression
Larmor magnetization ρ_a/r	$1.02\dfrac{T_a^{1/2}A_a^{1/2}}{Z_aBr}$
e Hall parameter Ω_e/ν_{ea}	$0.095\dfrac{T_e^{3/2}B}{Z_an_e\ln(\Lambda_{ea})}$
Transport timescale $\tau_{ab,eq}$	$9.71\times10^{-5}\dfrac{r^2n_eZ_aZ_b^2\ln(\Lambda_{ab})}{T_a^{5/2}}\times\left(\dfrac{A_aA_b}{A_a+A_b}\right)^{1/2}\left(1+\dfrac{\Omega_b^2}{\nu_{ba}^2}\right)s$
Ion Hall parameter Ω_a/ν_{ab}	$4.64\times10^{-3}\dfrac{T_a^{3/2}B}{Z_aZ_b^2n_b\ln(\Lambda_{ab})}\left(\dfrac{A_aA_b}{A_a+A_b}\right)^{-1/2}$

Relevant plasma parameters are summarized in Table I. Well-diagnosed implosion experiments like those undertaken at the Weizmann Institute might provide possible venues for pursuing these strategies.[57–70] These conditions need not be satisfied at all times during the implosion, but should be simultaneously satisfied at least at some point to observe the variation of impurity density over the length scale r. The condition on the multi-ion transport timescale can be somewhat relaxed if it is enough to observe the tendency of impurity ions to move radially in or out. However, in that case the size of the effect is going to be proportional to $\tau_{imp}/\tau_{ab,eq}$. In order to observe the difference between two impurities of different species, ion Hall parameter should be less than 1 for one impurity species and more than 1 for another impurity species. In practice, it can be done by having one of the impurity species to be at low density (as low as observation capabilities allow).

Observing radial collisional transport will be easier at stagnation or late in the compression phase rather than early in the compression phase due to the following consideration. Suppose for simplicity that the implosion obeys uniform radial compression with convergence ratio $C = r_0/r$ of a cylindrical plasma column which has adiabatic index γ. Then plasma parameters in the fuel have the following scaling: $n \propto C^2$, $T \propto n^{\gamma-1} \propto C^{2(\gamma-1)}$, $B \propto C^2$. Gyrofrequencies and collisional frequencies have $\Omega_s \propto C^2$ and $\nu_{ss'} \propto n/T^{3/2} \propto C^{5-3\gamma}$ scaling, respectively. Dimensionless parameters that characterize magnetization in various ways have the following scalings: $\beta \propto nT/B^2 \propto C^{2(\gamma-2)}$, $\Omega_a/\nu_{ab} \propto C^{3(\gamma-1)}$, $\rho_a/r \propto T^{1/2}B^{-1}r^{-1} \propto C^{\gamma-2}$. As such, the plasma becomes more collisionally magnetized during the implosion. In the collisionally unmagnetized plasma limit $\tau_{ab,eq} \propto r^2\nu_{ab}/v_{th}^2 \propto C^{-5(\gamma-1)}$; in the collisionally magnetized plasma limit $\tau_{ab,eq} \propto r^2/(\nu_{ab}\rho_b^2) \propto C^{\gamma-1}$.

Collisional radial transport of heavy impurities in a Z-pinch implosion occurs in stages. Initially, even after the axial magnetic field is applied, the plasma is still collisionally unmagnetized ($\Omega_a/\nu_{ab} \ll 1$) and the transport timescale $\tau_{ab,eq}$ is too slow compared to the implosion time for collisional multi-ion transport to dominate. Then, as the implosion progresses, $\tau_{ab,eq}$ drops dramatically ($\propto C^{-10/3}$ if $\gamma = 5/3$). Therefore, impurities start to be drawn into the hotspot due to temperature gradients and expelled from the hotspot due to density gradients. Then, when plasma becomes partially magnetized and, afterward, collisionally magnetized, the generalized pinch effect flips sign. Therefore, heavy ion impurities are expelled from the hotspot both due to temperature and density gradients, as the hotspot is both hotter and less dense than the surrounding plasma. The ion–ion transport timescale is sufficiently fast for the impurities to be expelled. After that, $\tau_{ab,eq}$ starts to increase. Hence, signatures of multi-ion collisional transport will be most prominent at stagnation.

V. PARTIAL-IONIZATION DECONFINEMENT EFFECT

Plasma where ions can be in multiple charge states exhibits yet another kind of transport behavior. For the purpose of multi-ion transport it can be treated as a combination of interacting fluids, each fluid being a collection of ions in a given charge state. These fluids can transform into one another via ionization or recombination. Therefore, each charge state fluid is evolving on both the ionization–recombination timescale and on the transport timescale. Once combined, these processes lead to the following effect, which is uniquely peculiar to partially ionized plasma. The difference is captured in Fig. 3.

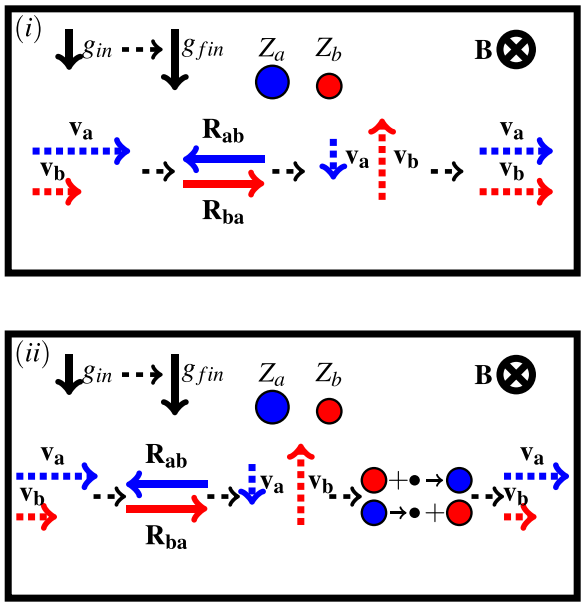

FIG. 3. Transport in fully ionized and partially ionized plasma. In fully ionized plasma (i) imbalance in flow velocities leads to ion–ion friction and corresponding cross-field transport. Due to this process ion densities adjust as to relax the difference of flow velocities. In partially ionized plasma (ii), once ions in a charge state move across field lines due to ion–ion friction, they ionize or recombine in order to maintain local charge state equilibrium. Consequently, densities of ion fluids are no longer independent. Because the drift velocities are thus constrained, the plasma must move as a whole.

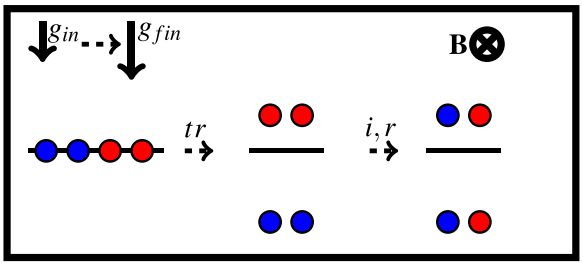

FIG. 4. Sedimentation in partially ionized plasma.

Suppose that a plasma slab is acted upon by an external force. Then, the equilibration process, which is depicted in Fig. 4, proceeds as follows. Ions in different charge states initially have different drift velocities. Therefore, when the ions in different charge states undergo elastic collisions, they change their position (first process in Fig. 4). After these ions move across magnetic field lines, they find themselves out of local charge state equilibrium. Therefore, some additional ionization or recombination happens to bring the plasma back to charge state equilibrium. However, because one process conserves net ion charge density, and another process conserves ion density, the net effect is that the plasma moves as a whole across magnetic field lines. This interplay is the partial-ionization deconfinement effect. It happens on the ion–ion transport timescale, which is $\mathcal{O}(\sqrt{m_i/m_e})$ faster than the deconfinement of fully ionized plasma, which in turn happens on the electron–ion transport timescale.

The partial-ionization deconfinement effect highlights the importance of treating each charge state separately. The combination of ionization, recombination, and cross-field transport allows for a new kind of plasma behavior, which would be impossible if only one of these mechanisms were present in the plasma.

Additionally, the partial-ionization deconfinement effect provides a first step toward a first-principle description of plasma transport when multiple charge states are allowed. Transitions between multiple charge states, coupled with cross-field transport, could change the nature of transport yet again, which would be of great interest to all kinds of laboratory plasmas where high-Z impurities are present.

VI. CONCLUSIONS

Plasma, due to its nature, allows rich physics. When multiple ion species are taken into account, new effects can be uncovered. In this paper, a few of these effects are highlighted. The first of them is a heat pump effect, which happens in fully ionized and magnetized plasma when an external (e.g., centrifugal) potential is applied to the plasma. The second is the pinch reversal effect, a change in the direction of cross-field heavy impurity transport in a Z-pinch in the later stages of implosion as plasma becomes collisionally magnetized. The third is the partial-ionization deconfinement effect, which shows that the interplay between cross-field transport, ionization, and recombination can lead to motion of plasma across magnetic field lines if there are ions in different charge states. Although a multitude of effects is described in this paper, the list of effects in this paragraph is not exhaustive. Because the phenomena described in this paper are inherent to plasma with multiple ion species, they provide an incentive to develop multi-ion fluid codes such as MITNS.[71]

Another interesting observation is that multi-ion transport effects can be studied using at least two different approaches. One of them is to start with multi-fluid equations and analyze them. The effects discussed in this paper can be inferred from momentum equations. Energy fluid equations can also help to uncover new effects, such as the drift-energy replacement effect.[72]

However, there is another approach. In the absence of temperature gradients, plasma obeys a maximum-entropy principle. It has been proved in Ref. 28 that, combined with the constraint on moving charge across magnetic field lines and a constraint on which species can move at the given timescale, the generalized pinch relations are recovered. This is a profound result, because the momentum equation, and the friction force between species in particular, can have quite a different form in various plasmas (in particular, it depends on Hall parameter). In the presence of temperature gradients, entropy itself is no longer maximized. However, consideration of the Onsager linear-response matrix still makes it possible to use entropy and thermodynamic techniques to infer the relationship between ion densities.[29] These results show that extending entropy-based fluid code development, e.g., in Refs. 73–77, to multi-ion-fluid systems could be of interest.

There are multiple future directions that could develop from uncovering these new curious cross-field transport effects. We will list a few possibilities. The first direction is to verify partial magnetization and partial ionization results experimentally. One configuration of interest is an appropriate diagnosed Z-pinch experiment, where impurity density can be adjusted and tracked, based on ideas in Sec. IV. Linear plasma devices might be a test bed to observe the partial-ionization deconfinement effect.

The second direction is to develop a theory of transport in partially ionized plasma with two charge states in the presence of background species. This could be of great interest to magnetic confinement devices, as high-Z impurity transport can be described in these terms.

The third direction is to develop a theory of partially ionized plasma with three and more charge states. In contrast to the case of two-charge-state plasma, once there are three and more charge states, the equilibrium is not guaranteed to be a local charge state equilibrium in the presence of temperature gradient. As such, cross-field transport could impact spectroscopic inferences in this case once charge states are not in local charge state equilibrium. Therefore, it could be of great interest to find out the size of this effect.

The fourth direction is to incorporate a simple model of cross-field transport into the codes which determine charge state equilibrium and estimate the impact of transport in that way.

The fifth direction is to build upon the results of Sec. V to try to explain relationship between transport coefficients in neoclassical or turbulent impurity transport from first principles. This lengthy list is a testament to the richness of cross-field transport physics in magnetized, multi-ion plasma, some of which has been explored recently and summarized here.

ACKNOWLEDGMENTS

The authors thank E. J. Kolmes, I. E. Ochs, T. Rubin, and A. Glasser for useful conversations. This work was supported by NSF Grant No. PHY-2308829 and by the NNSA Stewardship Science Academic Programs under U.S. Department of Energy Cooperative Agreement No. DE-NA0004148.

AUTHOR DECLARATIONS

Conflict of Interest

The authors have no conflicts to disclose.

Author Contributions

M. E. Mlodik: Conceptualization (equal); Formal analysis (lead); Investigation (lead); Software (equal); Validation (equal); Visualization (lead); Writing – original draft (lead). **N. J. Fisch:** Formal analysis (supporting); Funding acquisition (lead); Investigation (supporting); Project administration (lead); Software (equal); Supervision (lead); Validation (lead); Writing – original draft (supporting); Writing – review & editing (lead).

DATA AVAILABILITY

Data sharing is not applicable to this article as no new data were created or analyzed in this study.

REFERENCES

[1]M. E. Mlodik, E. J. Kolmes, I. E. Ochs, and N. J. Fisch, Phys. Rev. E **102**, 013212 (2020).
[2]M. E. Mlodik, E. J. Kolmes, I. E. Ochs, and N. J. Fisch, Phys. Plasmas **28**, 052702 (2021).
[3]M. E. Mlodik, E. J. Kolmes, I. E. Ochs, T. Rubin, and N. J. Fisch, Phys. Plasmas **29**, 112111 (2022).
[4]F. L. Hinton, "Collisional transport in plasma," in *Basic Plasma Physics*, edited by M. N. Rosenbluth and R. Z. Sagdeev (North-Holland Publishing Co., 1983), Vol. 1, Chap. 5, p. 147.
[5]P. Helander and D. J. Sigmar, *Collisional Transport in Magnetized Plasmas* (Cambridge University Press, Cambridge, UK, 2002).
[6]G. Kagan and X.-Z. Tang, Phys. Plasmas **21**, 022708 (2014).
[7]A. L. Velikovich, J. L. Giuliani, and S. T. Zalesak, Phys. Plasmas **22**, 042702 (2015).
[8]A. L. Velikovich, J. L. Giuliani, and S. T. Zalesak, Phys. Plasmas **26**, 112702 (2019).
[9]J. B. Taylor, Phys. Fluids **4**, 1142 (1961).
[10]S. I. Braginskii, "Transport processes in a plasma," in *Reviews of Plasma Physics*, edited by M. A. Leontovich (Consultants Bureau, New York, 1965), Vol. 1, p. 205.
[11]L. Spitzer, Astrophys. J. **116**, 299 (1952).
[12]E. J. Kolmes, I. E. Ochs, and N. J. Fisch, Phys. Plasmas **25**, 032508 (2018).
[13]B. Bonnevier, Plasma Phys. **13**, 763 (1971).
[14]J. W. Connor, Plasma Phys. **15**, 765 (1973).
[15]P. H. Rutherford, Phys. Fluids **17**, 1782 (1974).
[16]F. L. Hinton and T. B. Moore, Nucl. Fusion **14**, 639 (1974).
[17]T. M. O'Neil, Phys. Fluids **24**, 1447 (1981).
[18]S. P. Hirshman and D. J. Sigmar, Nucl. Fusion **21**, 1079 (1981).
[19]M. Krishnan, M. Geva, and J. L. Hirshfield, Phys. Rev. Lett. **46**, 36 (1981).
[20]M. Krishnan, Phys. Fluids **26**, 2676 (1983).
[21]H. Imajo, K. Hayasaka, R. Ohmukai, U. Tanaka, M. Watanabe, and S. Urabe, Phys. Rev. A **55**, 1276 (1997).
[22]D. H. E. Dubin and T. M. O'Neil, Rev. Mod. Phys. **71**, 87 (1999).
[23]E. Viezzer, T. Pütterich, E. Fable, A. Bergmann, R. Dux, R. M. McDermott, R. M. Churchill, and M. G. Dunne, Plasma Phys. Controlled Fusion **55**, 124037 (2013).
[24]C. Angioni and P. Helander, Plasma Phys. Controlled Fusion **56**, 124001 (2014).
[25]D. A. Dolgolenko and Y. A. Muromkin, Phys.-Usp. **60**, 994 (2017).
[26]S. J. Zweben, R. Gueroult, and N. J. Fisch, Phys. Plasmas **25**, 090901 (2018).
[27]C. Angioni, Plasma Phys. Controlled Fusion **63**, 073001 (2021).
[28]E. J. Kolmes, I. E. Ochs, M. E. Mlodik, and N. J. Fisch, Phys. Lett. A **384**, 126262 (2020).

[29]E. J. Kolmes, I. E. Ochs, M. E. Mlodik, and N. J. Fisch, Phys. Lett. A **447**, 128298 (2022).
[30]B. Lehnert, Nucl. Fusion **11**, 485 (1971).
[31]T. Ohkawa and R. L. Miller, Phys. Plasmas **9**, 5116 (2002).
[32]A. J. Fetterman and N. J. Fisch, Phys. Plasmas **18**, 094503 (2011).
[33]R. Gueroult and N. J. Fisch, Phys. Plasmas **19**, 122503 (2012).
[34]R. Gueroult and N. J. Fisch, Plasma Sources Sci. Technol. **23**, 035002 (2014).
[35]R. Gueroult, J.-M. Rax, and N. J. Fisch, J. Clean. Prod. **182**, 1060 (2018).
[36]A. P. Oiler, R. A. Usmanov, N. N. Antonov, A. V. Gavrikov, and V. P. Smirnov, Plasma Phys. Rep. **50**, 588 (2024).
[37]A. Fruchtman and G. Makrinich, Phys. Plasmas **31**, 043502 (2024).
[38]G. Liziakin, N. Antonov, V. S. Smirnov, R. Timirkhanov, A. Oiler, R. Usmanov, A. Melnikov, N. Vorona, S. Kislenko, A. Gavrikov, and V. P. Smirnov, J. Phys. D:Appl. Phys. **54**, 414005 (2021).
[39]A. V. Timofeev, Phys-Usp. **57**, 990 (2014).
[40]S. Shinohara and S. Horii, Jpn. J. Appl. Phys. **46**, 4276 (2007).
[41]J.-M. Rax and R. Gueroult, J. Plasma Phys **82**, 595820504 (2016).
[42]J. R. Davies, H. Wen, J.-Y. Ji, and E. D. Held, Phys. Plasmas **28**, 012305 (2021).
[43]J. D. Sadler, C. A. Walsh, and H. Li, Phys. Rev. Lett. **126**, 075001 (2021).
[44]A. N. Simakov, Phys. Plasmas **29**, 022304 (2022).
[45]N. A. Lopez, Phys. Plasmas **31**, 014701 (2024).
[46]M. H. Redi, S. A. Cohen, and E. J. Synakowski, Nucl. Fusion **31**, 1689 (1991).
[47]S. Braun and P. Helander, Phys. Plasmas **17**, 072514 (2010).
[48]I. E. Ochs and N. J. Fisch, Phys. Rev. Lett. **121**, 235002 (2018).
[49]I. E. Ochs and N. J. Fisch, Phys. Plasmas **25**, 122306 (2018).
[50]P. F. Knapp, M. R. Gomez, S. B. Hansen, M. E. Glinsky, C. A. Jennings, S. A. Slutz, E. C. Harding, K. D. Hahn, M. R. Weis, M. Evans, M. R. Martin, A. J. Harvey-Thompson, M. Geissel, I. C. Smith, D. E. Ruiz, K. J. Peterson, B. M. Jones, J. Schwarz, G. A. Rochau, D. B. Sinars, R. D. McBride, and P.-A. Gourdain, Phys. Plasmas **26**, 012704 (2019).
[51]M. R. Gomez, S. A. Slutz, P. F. Knapp, K. D. Hahn, M. R. Weis, E. C. Harding, M. Geissel, J. R. Fein, M. E. Glinsky, S. B. Hansen, A. J. Harvey-Thompson, C. A. Jennings, I. C. Smith, D. Woodbury, D. J. Ampleford, T. J. Awe, G. A. Chandler, M. H. Hess, D. C. Lamppa, C. E. Myers, C. L. Ruiz, A. B. Sefkow, J. Schwarz, D. A. Yager-Elorriaga, B. Jones, J. L. Porter, K. J. Peterson, R. D. McBride, G. A. Rochau, and D. B. Sinars, IEEE Plasma Sci. **47**, 2081 (2019).
[52]P. F. Schmit, P. F. Knapp, S. B. Hansen, M. R. Gomez, K. D. Hahn, D. B. Sinars, K. J. Peterson, S. A. Slutz, A. B. Sefkow, T. J. Awe, E. Harding, C. A. Jennings, G. A. Chandler, G. W. Cooper, M. E. Cuneo, M. Geissel, A. J. Harvey-Thompson, M. C. Herrmann, M. H. Hess, O. Johns, D. C. Lamppa, M. R. Martin, R. D. McBride, J. L. Porter, G. K. Robertson, G. A. Rochau, D. C. Rovang, C. L. Ruiz, M. E. Savage, I. C. Smith, W. A. Stygar, and R. A. Vesey, Phys. Rev. Lett. **113**, 155004 (2014).
[53]S. A. Slutz and R. A. Vesey, Phys. Rev. Lett. **108**, 025003 (2012).
[54]M. R. Gomez, S. A. Slutz, A. B. Sefkow, D. B. Sinars, K. D. Hahn, S. B. Hansen, E. C. Harding, P. F. Knapp, P. F. Schmit, C. A. Jennings, T. J. Awe, M. Geissel, D. C. Rovang, G. A. Chandler, G. W. Cooper, M. E. Cuneo, A. J. Harvey-Thompson, M. C. Herrmann, M. H. Hess, O. Johns, D. C. Lamppa, M. R. Martin, R. D. McBride, K. J. Peterson, J. L. Porter, G. K. Robertson, G. A. Rochau, C. L. Ruiz, M. E. Savage, I. C. Smith, W. A. Stygar, and R. A. Vesey, Phys. Rev. Lett. **113**, 155003 (2014).
[55]Y. Kim, H. W. Herrmann, N. M. Hoffman, M. J. Schmitt, G. Kagan, A. M. McEvoy, A. B. Zylstra, J. M. Smidt, S. Gales, A. Leatherland, M. Rubery, M. Gatu Johnson, J. A. Frenje, V. Y. Glebov, and C. Forrest, Phys. Plasmas **28**, 012707 (2021).
[56]A. J. Harvey-Thompson, M. R. Weis, E. C. Harding, M. Geissel, D. J. Ampleford, G. A. Chandler, J. R. Fein, M. E. Glinsky, M. R. Gomez, K. D. Hahn, S. B. Hansen, C. A. Jennings, P. F. Knapp, R. R. Paguio, L. Perea, K. J. Peterson, J. L. Porter, P. K. Rambo, G. K. Robertson, G. A. Rochau, D. E. Ruiz, J. Schwarz, J. E. Shores, D. B. Sinars, S. A. Slutz, G. E. Smith, I. C. Smith, C. S. Speas, and K. Whittemore, Phys. Plasmas **25**, 112705 (2018).
[57]M. E. Foord, Y. Maron, G. Davara, L. Gregorian, and A. Fisher, Phys. Rev. Lett. **72**, 3827 (1994).
[58]G. Davara, L. Gregorian, E. Kroupp, and Y. Maron, Phys. Plasmas **5**, 1068 (1998).
[59]L. Gregorian, V. A. Bernshtam, E. Kroupp, G. Davara, and Y. Maron, Phys. Rev. E **67**, 016404 (2003).
[60]L. Gregorian, E. Kroupp, G. Davara, A. Starobinets, V. I. Fisher, V. A. Bernshtam, Y. V. Ralchenko, Y. Maron, A. Fisher, and D. H. H. Hoffmann, Phys. Rev. E **71**, 056402 (2005).
[61]L. Gregorian, E. Kroupp, G. Davara, V. I. Fisher, A. Starobinets, V. A. Bernshtam, A. Fisher, and Y. Maron, Phys. Plasmas **12**, 092704 (2005).
[62]E. Stambulchik, K. Tsigutkin, and Y. Maron, Phys. Rev. Lett. **98**, 225001 (2007).
[63]R. Doron, D. Mikitchuk, C. Stollberg, G. Rosenzweig, E. Stambulchik, E. Kroupp, Y. Maron, and D. A. Hammer, High Energy Density Phys. **10**, 56 (2014).
[64]R. Doron, B. Rubinstein, J. Citrin, R. Arad, Y. Maron, A. Fruchtman, H. R. Strauss, and T. A. Mehlhorn, Phys. Plasmas **23**, 122126 (2016).
[65]D. Alumot, E. Kroupp, E. Stambulchik, A. Starobinets, I. Uschmann, and Y. Maron, Phys. Rev. Lett. **122**, 095001 (2019).
[66]D. Mikitchuk, M. Cvejić, R. Doron, E. Kroupp, C. Stollberg, Y. Maron, A. L. Velikovich, N. D. Ouart, J. L. Giuliani, T. A. Mehlhorn, and E. Yu, Phys. Rev. Lett. **122**, 045001 (2019).
[67]G. Rosenzweig, E. Kroupp, T. Queller, A. Starobinets, Y. Maron, V. Tangri, J. L. Giuliani, and A. Fruchtman, Phys. Plasmas **27**, 022705 (2020).
[68]Y. Maron, Phys. Plasmas **27**, 060901 (2020).
[69]M. Cvejić, D. Mikitchuk, E. Kroupp, R. Doron, P. Sharma, Y. Maron, A. L. Velikovich, A. Fruchtman, I. E. Ochs, E. J. Kolmes, and N. J. Fisch, Phys. Rev. Lett. **128**, 015001 (2022).
[70]Y. Maron, R. Doron, M. Cvejić, E. Stambulchik, D. Mikitchuk, C. Stollberg, T. Queller, E. Kroupp, G. Rosenzweig, B. Rubinstein, S. Biswas, V. Bernshtam, O. Nedostup, V. Litmanovich, V. Fisher, A. Starobinets, A. Fruchtman, A. Fisher, V. Tangri, J. L. Giuliani, A. L. Velikovich, A. Dasgupta, I. E. Ochs, E. J. Kolmes, M. E. Mlodik, S. Davidovits, N. J. Fisch, and M. D. Johnston, IEEE Trans. Plasma Sci. **51**, 3407 (2023).
[71]E. J. Kolmes, I. E. Ochs, and N. J. Fisch, Comput. Phys. Commun. **258**, 107511 (2021).
[72]M. E. Mlodik, E. J. Kolmes, and N. J. Fisch, arXiv:2405.05829 [physics.plasm-ph] (2024).
[73]R. Abgrall and H. Kumar, J. Sci. Comput. **60**, 584 (2014).
[74]R. Abgrall, J. Comput. Phys. **372**, 640 (2018).
[75]R. Abgrall, P. Öffner, and H. Ranocha, J. Comput. Phys. **453**, 110955 (2022).
[76]R. Abgrall, S. Busto, and M. Dumbser, Appl. Math. Comput. **440**, 127629 (2023).
[77]W. Boscheri, M. Dumbser, and P.-H. Maire, SIAM J. Sci. Comput. **46**, A2224 (2024).